

Frequency measurements and self-broadening of sub-Doppler transitions in the $v_1 + v_3$ band of C_2H_2

Sylvestre Twagirayezu,^{1, a)} Gregory E. Hall,^{1, b)} and Trevor J. Sears^{1, 2, c)}

¹⁾*Division of Chemistry, Department of Energy and Photon Sciences, Brookhaven National Laboratory, Upton, NY 11973-5000, USA*

²⁾*Chemistry Department, Stony Brook University, Stony Brook, NY 11794-3400, USA*

(Dated: 10 March 2020)

Frequency comb-referenced measurements of sub-Doppler laser saturation dip absorption lines in the $v_1 + v_3$ band of acetylene near $1.5 \mu\text{m}$ are reported. These measurements include transitions involving higher rotational levels than previously frequency measured in this band. The accuracy of the measured frequencies is typically better than 10 kHz. Measurements of the observed sub-Doppler line widths as a function of pressure showed that the self pressure-broadening coefficients are about 3.5 times larger than those derived from conventional pressure broadening of unsaturated Doppler-limited spectra. This is attributed to the contribution of velocity-changing collisions to the total dephasing rate in the low pressure sub-Doppler measurements. At higher pressures, when the homogeneous broadening becomes comparable to the typical Doppler shift per elastic collision, the velocity changing collisions cease to contribute significantly to the incremental pressure broadening. A time-dependent soft collision model is developed to illustrate the transition between low and high pressure regimes of sub-Doppler pressure-broadening.

^{a)}Electronic mail: stwagirayezu@lamar.edu; Present Address: Department of Chemistry & Biochemistry, Lamar University, Beaumont, TX 77710

^{b)}Electronic mail: gehall@bnl.gov

^{c)}Electronic mail: trevor.sears@stonybrook.edu

I. INTRODUCTION

The $v_1 + v_3$ band of acetylene, C_2H_2 , is a strong vibrational combination band in the $1.5\mu m$ region of the spectrum. It is a parallel band with a simple P- ($\Delta J = -1$) and R- ($\Delta J = +1$) branch rotational structure and has long been used as a secondary wavelength, and more recently¹ frequency, standard. Techniques for the routine frequency-measurement of optical spectra have opened the way to far more precise determinations of line positions and shapes^{2,3} than were previously available. We have previously frequency-measured hot band lines in this spectrum for the purposes of calibrating Doppler- and pressure-broadened measurements.⁴ These measurements were made using laser saturation dip spectroscopy with a fiber laser-amplified *c.w.* extended cavity diode laser referenced to a frequency comb as the source.

Here, we report rest frequency measurements for some lines in the spectrum that have not previously been frequency measured.¹ During the frequency measurements, it was noted that the width of the saturation resonance varied with pressure, in a similar way to that seen in a conventional absorption spectrum. The pressure and power dependence of the saturation dips have been measured and analyzed. The pressure broadening coefficients are typically about 3.5 times larger than those previously reported from conventional, Doppler-limited, spectroscopic measurements at much higher pressures. Previous measurements of sub-Doppler saturation dip spectra in atoms such as Xe^{5,6} and others discussed in section IV also report self-pressure broadening coefficients larger than seen in Doppler broadened spectra. Multiple observations, see for example references,⁷⁻⁹ of sub-Doppler spectra of methane in the $3.39\ \mu m$ lasing transition have also been reported and these also exhibit larger self-pressure-broadening coefficients. Measurements of sub-Doppler CO_2 vibration-rotation transitions¹⁰⁻¹² also show larger self-broadening than observed in Doppler-limited spectra

The interpretation of these and other similar observations has generally focussed on the effects of velocity-changing collisions. Physically, this is reasonable as sub-Doppler spectroscopy, in which a single velocity group of molecules is selected, might be expected to be more sensitive to weak, large cross section, collisions compared to Doppler-limited spectra where the line width is determined by the ensemble average of all velocities in the sample. In the spirit of these ideas, we describe a simple collisional model based on a soft

collision model^{13,14} and the interplay between damping and dephasing, which mimics the observations.

II. EXPERIMENTAL

Sub-Doppler spectra of selected ro-vibrational lines in the $\nu_1 + \nu_3$ band of acetylene were measured by the transmission of an external cavity diode laser beam through a resonant cavity containing low pressures of acetylene. The probe laser beam was locked to a cavity resonance using the Pound-Drever-Hall method,¹⁵ with a DC-300 kHz error correction signal added directly to the diode injection current. The resonant cavity consisted of two highly-reflective mirrors, each mounted on a PZT piezo-electric actuator. One actuator with a slow response, but longer travel was used for coarse positioning of the cavity modes, the second with short travel, but higher frequency response executed an 830 Hz dither in addition to a stepwise ramp scan, generated by a second feedback loop that controlled the offset frequency between the probe laser and a reference tooth of the frequency comb. With both feedback loops locked, the repetition rate of the frequency comb was stepped to change the average optical frequency of the synchronously dithered probe laser and sample cavity transmission maximum through the sub-Doppler resonance. Data were recorded using an optical frequency step size of approximately 70 kHz through the center of each line, with steps three times larger elsewhere, to accelerate the data acquisition. Each data point was typically averaged for 3s with a 300ms output time constant for the lock-in amplifier. A programmed delay was included after each frequency step to allow the system to stabilize before data acquisition began. More complete details have been previously reported.^{4,16}

As detailed below, the data analysis was carried out assuming a Voigt-type profile to account for a combination of transit-time and pressure-broadening effects. The (narrow) transit-time contribution to the observations is most important for the lower pressure measurements and an analysis of the effect of changing the width of the Gaussian component is included in Supplementary Information for this paper.

We found the line shape modeling required a pressure-independent Lorentzian component to the line shape function, that could not be attributed to the effect of wavelength modulation broadening.^{17,18} Instead, this residual broadening is mostly due to fluctuations of the probe laser frequency derived from mechanical and acoustical noise sources. The av-

erage laser frequency was accurately maintained by reference to the frequency comb, but the bandwidth of the phase lock loop holding the absolute comb frequency was slow enough that measured data points were an average over a Lorentzian distribution of frequencies centered about the exact center one. The 830 Hz component of the fluctuations was demodulated by the detection system. We have modeled the effect quantitatively by assuming a Lorentzian distribution of frequency noise on top of 1-f wavelength modulation of a Voigt line shape. The convolution of two Lorentzian functions, *i.e.* frequency noise plus a pressure-dependent broadening, leads to a new Lorentzian function with width parameter, γ , equal to the sum of the widths of the two constituents. The modeling also showed that the modulation-induced broadening was small, and its effects were confined to the Gaussian, transit-time, contribution to the Voigt line shape, implying the actual transit time broadening was somewhat smaller than derived below.

III. RESULTS

A. Pressure-dependent line profiles

Sub-Doppler resonances for the P(31) line at several pressures are shown in Figure 1. In a low intensity limit, where the power broadening is negligible, the observed saturation dip line shape can be treated as the convolution of a Gaussian component due to transit-time broadening^{19–23} and a Lorentzian component due to multiple damping and dephasing mechanisms. The transit-time broadening depends on the laser beam size and the distribution of transverse velocities in the molecular sample. Most models of the effect just include the most probable Maxwell-Boltzmann velocity, $u_p = \sqrt{\frac{2k_B T}{m}}$, although a more realistic description of the interaction would include the fact the slower molecules will contribute differently to faster ones²³ and a description of the 2-D velocity distribution perpendicular to the laser axis.²⁴ The convolution of the Gaussian and Lorentzian gives the well-known Voigt profile. With an estimated beam waist radius in the cavity of ≈ 0.5 mm and assuming the expression for transit-time broadening from Bordé and Hall,^{20–22} $\Delta\nu_{tt} \approx \frac{u_p}{8w_0}$ we estimate a Gaussian half-width-half-maximum (HWHM) of 0.112 MHz. In fact, an initial analysis of the P(31) data showed the Gaussian contribution to be constant over the pressure range studied, at approximately 0.105 MHz HWHM, which is very close to the estimate. We note that other

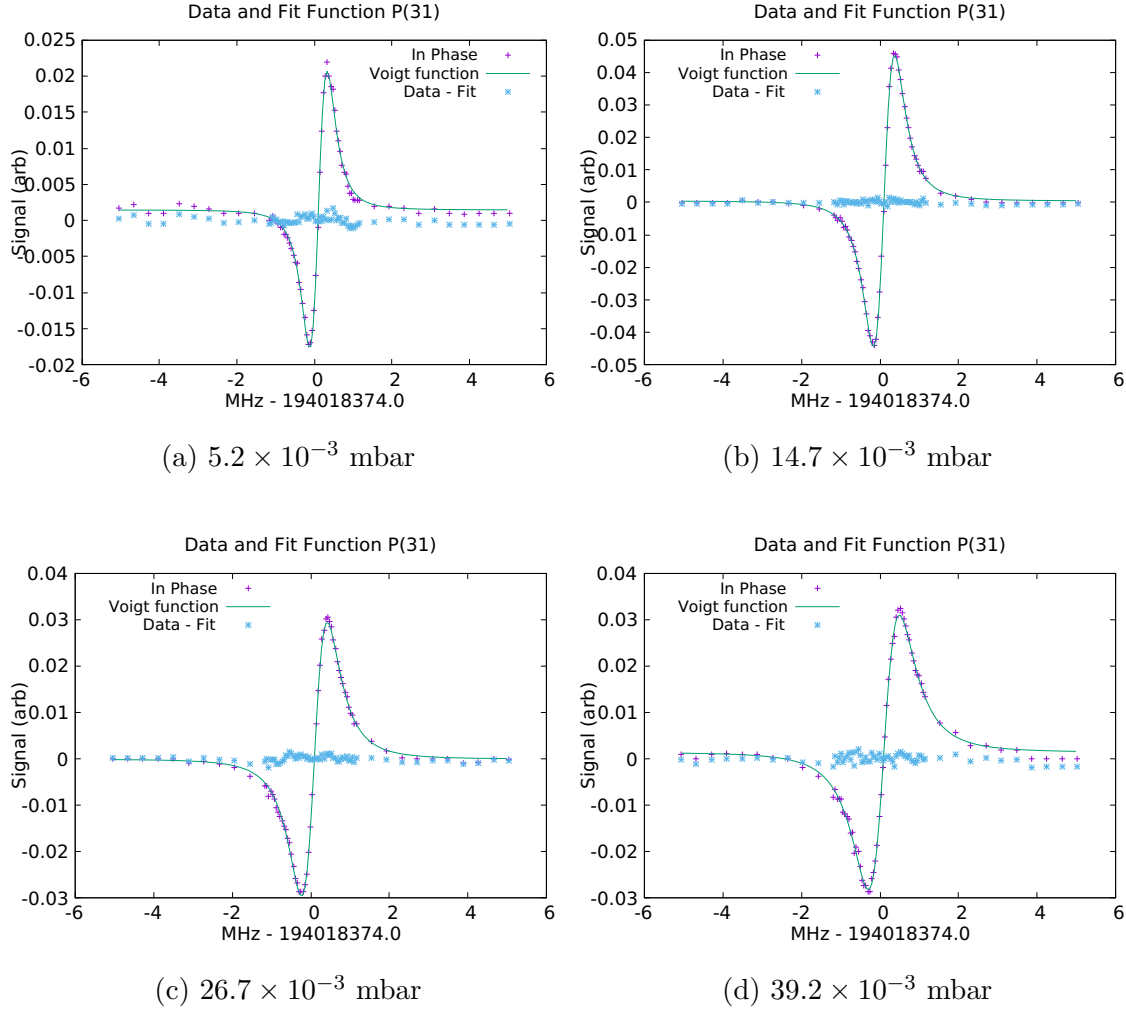


FIG. 1: Saturation dip spectra for the P(31) line in the $v_1 + v_3$ band of C_2H_2 at a series of sample pressures, shown in the subcaptions, 1 mbar=0.750062 Torr=100 Pa. Scans were recorded with a more dense sampling near line center. The increase in observed width with sample pressure is clear. All data were recorded at approximately 11 mW intracavity power. The line shapes were fit to a derivative of a Voigt profile consisting of a fixed Gaussian transit-time, and an adjustable Lorentzian component.

derived approximate forms for $\Delta\nu_{t}$ such as Demtroeder's¹⁹ $\frac{\sqrt{2\ln 2}}{2\pi} \frac{u_p}{w_0}$ do not agree as closely with the experiment. Since the data for transitions other than P(31) were less extensive and generally of poorer signal-to-noise, in all subsequent analysis the Gaussian contribution to the measurements was assumed to be constant and fixed to 0.105 MHz HWHM.

Voigt fits to the pressure-dependent P(31) line profiles with fixed Gaussian HWHM of 0.105 MHz lead to the Lorentzian broadening as plotted in Figure 2. The intercept in

Figure 2 is the extrapolated zero-pressure Lorentzian width, which corresponds to residual broadening due mainly to the mechanisms discussed above. The natural (fluorescence) lifetime for the upper level, $J = 30$ in the $v_1 + v_3$ level can be estimated from known Einstein A-factors.²⁵ It is approximately 50 Hz, too small to contribute significantly to the line widths. Power broadening was characterized in separate experiments in which data for P(31) were recorded at a pressure of 14.3×10^{-3} mbar at a series of intracavity laser powers. Over the range 11-40 mW, the HWHM increased linearly with a slope of $\gamma_{pwr} = 3.38(33)$ kHz/mW, suggesting the power broadening contribution to the spectra in Figure 1 is no more than 37 kHz. Hence, the instrumental broadening due to the effect discussed in section II is of the order of 230 kHz HWHM.

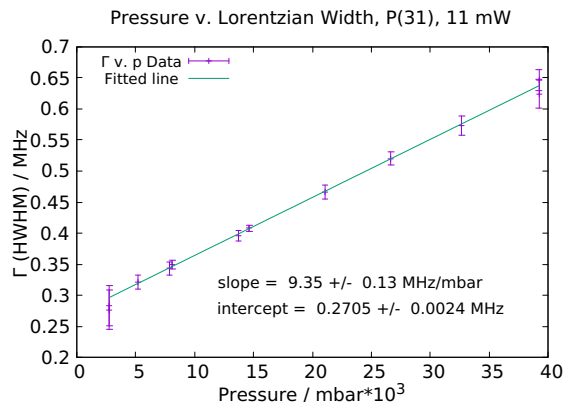


FIG. 2: Plot of Lorentzian width Γ for the P(31) saturation dip spectra in a Voigt fit with Gaussian HWHM fixed at 0.105 MHz. The values are well described by a linear model. The error bars on the points are three standard deviations of the fitted widths for the individual measurements.

The slope of the line in Figure 2, *i.e.* 9.35(13) MHz/mbar, or 12.46(17) MHz/Torr, is $\gamma_{self}(\text{HWHM})$: the self-broadening coefficient for the sub-Doppler P(31) transition at a one-way intracavity power of 11 mW. The cavity-defined, counter-propagating, single laser beam geometry in the present measurements means that they may be compared directly to $\gamma_{self}(\text{Doppler})$ derived from single-pass measurements of Doppler-broadened gaseous samples. The sub-Doppler γ_{self} determined here is about 3.5 times larger than $\gamma_{self}(\text{Doppler})$ for the same line. Forward- and backward-going beams address separate velocity groups, each lifetime broadened. The convolution of a tunable probe with a fixed-frequency depletion would lead to feature that is double the width of either one alone.⁸ However, this effect is exactly compensated in a single beam cavity measurement, since the relative Doppler de-

tuning of the forward and backward beams changes at twice the scan rate. There was some confusion on this topic in the early saturation dip literature,²⁶ when comparing pressure broadening of sub-Doppler features and Doppler-broadened spectra at higher pressures.

A series of saturation dip spectra at pressures from 2.9 to 29.4 mTorr ($(3.9 - 39.2) \times 10^{-3}$ mbar) for the P(31) - P(37) lines in the $v_1 + v_3$ band spectrum of acetylene were measured and analyzed. Table I summarizes the self pressure-broadening coefficients for sub-Doppler resonances in these transitions, along with literature values of the pressure broadening coefficients derived from Doppler-broadened spectra. All sub-Doppler coefficients are significantly larger than their Doppler-broadened counterparts and we also note that the change in γ_{self} measured here ($\approx 4\%$) over this limited range of rotational quantum numbers is significantly smaller than for conventional Doppler-limited spectra, where there is a 15% reduction from P(31) to P(35). These observations imply that different mechanisms are active in the two types of experimental measurements and we discuss this below. There is much current interest in differences between self pressure-broadening in ortho- and para-acetylene.^{27,28} Unfortunately, the estimated error in the self-broadening coefficient for the only para- line for which pressure broadening has been measured here, P(34), is too large to distinguish small ortho-/para- differences.

B. Rest frequencies

The rest frequencies determined for the observed rotational transitions are also summarized in Table I. The cited frequency uncertainties are the statistical (1σ) errors from multiple measurements of each line at various pressures between approximately 3 and 40×10^{-3} mbar. We noted a slight tendency towards a negative pressure-frequency shift coefficient for the P(31) data, $\Delta_0 = -0.34(16)$ MHz/mbar with one standard deviation in parenthesis. The estimated zero-pressure intercept from the fit of the P(31) data from this analysis was 194018374.106(3) MHz, *i.e.* slightly larger than quoted in Table I, but within the combined estimated $1-\sigma$ errors. For P(11), we previously determined $\Delta_0 = -0.4238(20)$ MHz/mbar from extensive Doppler-limited data.³ If the present rotational transitions had a similar pressure-dependent shift coefficient, the low-pressure shifts would be close to the accuracy and precision limits of our current measurements, leading to no conclusive comparison of high and low pressure shifting coefficients.

TABLE I: Frequencies and broadening parameters of selected transitions in the $\nu_1 + \nu_3$ band of C_2H_2 .

Transition	Frequency ^a	γ_{self} ^b	$\gamma_{self}(Doppler)$ ^c
	MHz	MHz/mbar	MHz/mbar
P(31)	194018374.101(3) ^d	9.35(13)	2.65
P(32)	193924561.231(6)		2.56
P(33)	193830012.907(3)	9.49(37)	2.45
P(34)	193734752.121(10)	7.3(3.1)	2.35
P(35)	193638764.411(6)	9.41(40)	2.24
P(36)	193542055.096(30)		2.13
P(37)	193444626.334(20)		2.02

^a Measured rest frequency from sub-Doppler spectroscopy (this work).

^b Sub-Doppler self-broadening coefficient (this work).

^c Doppler self-broadening coefficient, average of literature values.^{29,30}

^d Uncertainties in parenthesis are one standard deviation in units of the last quoted significant figures.

There have been relatively few direct comparisons of self-pressure shifts for the same transitions between Doppler-limited and sub-Doppler resonances. Recent very high precision measurements on sub-Doppler lines in the (3-0) band of carbon monoxide³¹ found an upper bound to the pressure shift of a few tenths kHz/mbar. A significantly larger CO self-shift of 0.16 to 0.31 MHz/Torr (120-230 kHz/mbar) was reported in Doppler and pressure broadened FTIR spectra.³² Sub-Doppler measurements on a methane transition at $3.39 \mu m$ ⁸ found an unmeasurably small (75 ± 150 Hz/Torr) self-pressure shift coefficient at low pressures, while conventional IR absorption methane spectra have been reported to have much larger self-pressure shifts of $-0.017 \text{ cm}^{-1} \text{ atm}^{-1}$ (-670 kHz/Torr) for transitions in the 6000 cm^{-1} region.³³ Other sub-Doppler IR measurements of carbon monoxide³⁴ and water³⁵ similarly led to upper bounds smaller than the high-pressure self-pressure shift. Precise measurements of saturation dip spectra of ethylene in the $10 \mu m$ region³⁶ and iodine³⁷ in the visible showed detectable, small self-shifts, but with a nonlinear pressure dependence. Self-collisional frequency shift coefficients for sub-Doppler HD overtone lines³⁸ were, however, found to be much larger at -900 kHz/mbar, some $10\times$ larger than found in Doppler-broadened spectra of the normal isotopomer, H_2 .³⁹ Overall then, there is little or no pressure-induced shift seen in most of the sub-Doppler experiments and theoretical consideration of this phenomenon in the literature is sparse or non-existent.

C. Time-Dependent Collisional Model

The influence of velocity-changing collisions (VCCs) on the widths of low-pressure sub-Doppler line profiles has been investigated by numerical evaluation of model electric field correlation functions, which detail the damping and dephasing that are responsible for the broadening of a resonant absorption, in the spirit of Galatry¹³ and Rautian and Sobel'man.¹⁴

The line profile is given by the real Fourier transform of the correlation function $\Phi(\tau)$:

$$I(\omega - \omega_0) = \frac{1}{\pi} \Re \int_0^\infty e^{i(\omega - \omega_0)\tau} \Phi(\tau) d\tau. \quad (1)$$

The total correlation function can be approximated as the product of an exponential damping function $\Phi_\gamma(\tau)$, a fly-out or transit time damping function $\Phi_{t_t}(\tau)$, and a velocity-dependent dephasing function $\Phi_v(\tau)$

$$\Phi(\tau) = \Phi_\gamma(\tau) \Phi_{t_t}(\tau) \Phi_v(\tau) \quad (2)$$

$$\Phi_\gamma(\tau) = e^{-\gamma\tau} \quad (3)$$

$$\Phi_{t_t}(\tau) = e^{-(\tau/t_t)^2} \quad (4)$$

$$\Phi_v(\tau) = \langle e^{-i\mathbf{k}\cdot\mathbf{r}(\tau)} \rangle \quad (5)$$

with

$$\mathbf{r}(\tau) = \int_t^{t+\tau} \mathbf{v}(t') dt'. \quad (6)$$

The damping rate γ is primarily a pressure-dependent inelastic damping rate but may also include a zero-pressure radiative contribution. The transit time contribution is approximated as a Gaussian function of time, with typical collisionless transit time, t_t . The Doppler effects due to a static or fluctuating velocity distribution are contained in the correlation function $\Phi_v(\tau)$, where the angle brackets in Eq.(5) denote an ensemble average. The motion of the absorber along the propagation direction of the light introduces a time-dependent phase, $\mathbf{k} \cdot \mathbf{r}(\tau)$. For time τ shorter than the time interval between collisions, the velocity \mathbf{v} is constant, and $\mathbf{r}(\tau) = \mathbf{v}\tau$. The phase, $\mathbf{k} \cdot \mathbf{r}(\tau)$, is then a linear function of time, corresponding to a fixed Doppler frequency offset of v/λ , with v the component of velocity along the wavevector \mathbf{k} . For a thermal sample with a low collision rate, the ensemble average of velocities gives a Gaussian correlation function as the low pressure limit of $\Phi_v(\tau)$. The

Fourier transform gives the usual Gaussian Doppler line profile, $I(\omega - \omega_0)$, for which the transit time damping is typically negligible compared to the rapid dephasing from multiple Doppler shifts. Including an additional exponential damping, through $\Phi_\gamma(\tau)$, leads to a Voigt profile. As the collision rate increases with pressure, each absorber may experience more than one Doppler-shifted frequency before suffering an inelastic collision or leaving the interaction region. In this case, the correlation function $\Phi_v(\tau)$ will dephase more slowly than the inhomogeneous average over multiple Doppler shifts, characterizing the narrowing associated with the velocity diffusion. The confinement at higher pressures makes Eq. (4) an increasingly inaccurate representation of transit time contributions, although a pressure-dependent increase in effective transit time only renders this slow damping an even more negligible contribution to the total correlation function at higher pressures.

For application to sub-Doppler line profiles, the inhomogeneous averaging over the thermal velocity distribution is left out, and only the resonantly selected velocity class of molecules with a specific initial Doppler shift is considered, while retaining the same treatment of velocity diffusion, inelastic loss of population, and the transit time.

The central point of the model is to depict the variable effect of velocity changing collisions with pressure, as the pressure-dependent homogeneous line width changes from small to large compared to the typical Doppler shifts accompanying an elastic collision. Relevant previous discussions of these questions can be found, for example, in several references from the early days of saturation spectroscopy.^{5,7,10,11,37}

Neglected in this model are any pressure shifts, collision effects in the excited state, properly treated with a density matrix approach, power broadening and the variation of the saturation parameter on the pressure, and any effects of radially variable intensities, wavefront curvature and recoil effects, all important in more quantitative treatments.^{6,24,40,41} The finite duration of the collisions is neglected by assuming a negligible phase shift during the collision. The speed-dependence of collision rates has also been neglected, as has any explicit treatment of residual broadening due to instrumental effects discussed above.

It is worth noting that the velocity change associated with inelastic collisions, while contributing substantially to the conventional diffusion constant and the overall translational thermalization rate, is irrelevant to pressure broadening, since the state change immediately removes the molecule from the near-resonantly driven ensemble under consideration. It is only the differential cross sections for elastic (state-preserving) collisions that need be

considered in the evaluation of $\Phi_v(\tau)$. When expressed as a laboratory-frame collision kernel, the forward peak in the elastic differential cross section leads to a cusp-like distribution of velocity change along a viewing direction.⁴²⁻⁴⁴ In the present numerical illustration, the collision kernel is approximated as a symmetric exponential function of the velocity change along the viewing direction:

$$A(v, v') \propto e^{-|v-v'|/\Delta_{vcc}} \quad (7)$$

with Δ_{vcc} the average absolute value of the velocity change following an elastic collision. This form of a collision kernel does not have the correct asymptotic form required to converge at long times to a Maxwell-Boltzmann velocity distribution, but it can quite accurately represent the first few elastic collisions with small total displacements in velocity space compared to the thermal velocity. Inelastic collisions truncate the sequence of elastic velocity changing collision long before thermalization, so that this failure to satisfy asymptotic reversibility is not a serious problem. Realistic calculations of elastic differential cross sections peak at scattering angles less than 2 degrees, which, when combined with the kinematic averaging of center of mass to laboratory frame velocity changes find typical Doppler shifts of a few MHz per collision for C_2H_2 transitions in the near infrared at room temperature.

With these simplifications, a numerical simulation based on Eq. (1-7) for the pressure-dependent sub-Doppler line profiles can be made with only three relevant parameters: the ratio of elastic to inelastic collision rates γ_e/γ , the typical Doppler shift per elastic collision Δ_{vcc}/λ , and a transit time t_t . In numerical calculations designed to mimic the conditions of the present acetylene measurements, the correlation function is evaluated with 100 ps time steps from 0 to 50 μs . The transit time contribution $\Phi_{t_t}(\tau)$ is evaluated with $t_t = 5\mu s$. The inelastic contribution $\Phi_\gamma(\tau)$ is evaluated with the damping rate $\gamma = 2\pi p \cdot 2.65 \times 10^6 \mu s^{-1} \text{ mbar}^{-1}$, with pressure p in mbar, chosen to match the experimental 2.65 MHz/mbar high-pressure self-broadening coefficient (HWHM) for a $J = 31$ line of C_2H_2 .^{29,30} The velocity-dependent correlation function $\Phi_v(\tau)$ is evaluated by a Monte Carlo procedure with one parameter for the elastic to inelastic collision ratio, γ_e/γ , and another to parameterize the typical magnitude of the velocity change per collision, Δ_{vcc} . For each time array in the ensemble average, the time array is partitioned into a sequence of collisionless intervals, $\{\Delta t_i\}$, with a random sample of times between elastic collisions generated from an exponential distribution with a mean value $\langle \Delta t \rangle = 1/\gamma_e$. For each molecular trajectory in the ensemble average, then, the phase factor $\mathbf{k} \cdot \mathbf{r}(\tau)$ in Eq (5) is a continuous, piecewise linear function of

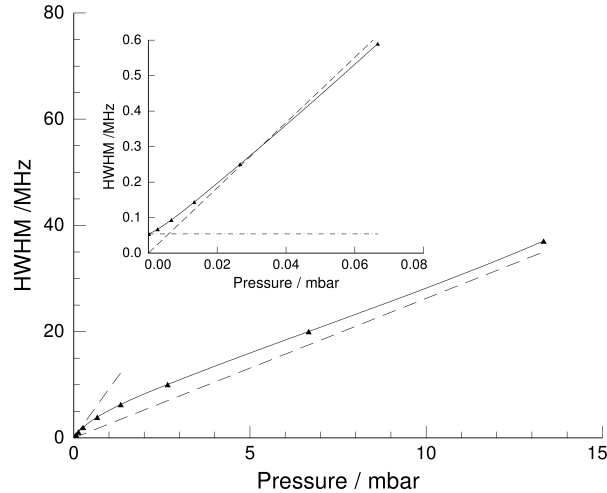


FIG. 3: Simulated pressure dependence of sub-Doppler line broadening. At pressures above 3 mbar, the HWHM increases with a slope characteristic of the inelastic rate. The steeper dashed line at lower pressures has a slope characteristic of the total elastic + inelastic rate. The low pressure inset shows the transit time limit as a horizontal dashed line, and the steeper sloped line from the main figure.

time, with a local slope in each collisionless time interval equal to the current detuning v_i/λ . The molecule follows a random walk in velocity $\{v_i\}$ starting at zero displacement from the laser-selected initial value. The velocity steps $v_{i+1} - v_i$ are sampled from the collision kernel, $A(v, v')$ of Eq (7), with Δ_{vcc}/λ set to 3 MHz. For the illustrations in Figures (3) and (4), γ_e/γ is set to 2.5. Demonstration code implementing this algorithm is available in the Supplemental Material for this paper in the form of a stand-alone Windows executable file and a LabView 2011 library.

Figure 3 shows the resulting trend in HWHM as a function of pressure, based on the Fourier transform of the simulated correlation function, using the model parameters above. Two limiting pressure regimes can be seen, with local slopes corresponding to the total collision rate at low pressure, and just the inelastic collision rate at high pressures. The transition between high and low pressure regimes occurs when the total pressure broadening is comparable to the Doppler shift per collision.

Figure 4 shows correlation functions at several pressures. In the low pressure region, the curvature in the plots of $\log \Phi(\tau)$ comes from the pressure-independent quadratic transit time contribution, which becomes negligible at higher pressures, when compared to the increasingly fast collision-induced damping. Throughout the pressure range below 0.05 mbar,

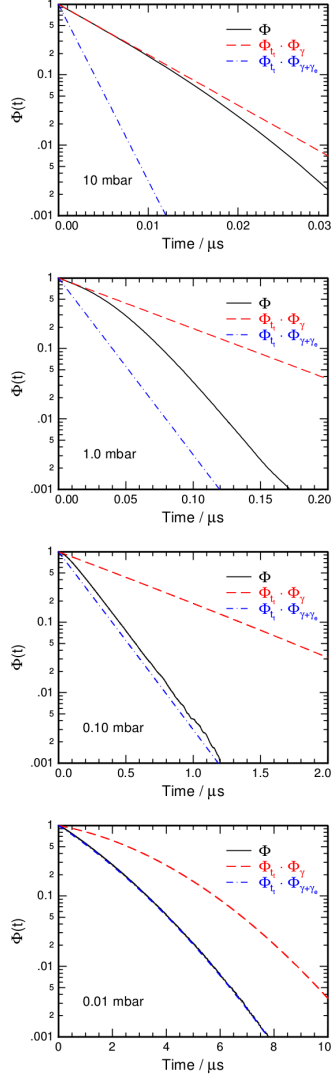


FIG. 4: Correlation functions computed from 0.01 to 10 mbar. Solid black lines are the full simulation, a product of $\Phi_\gamma(\tau)$, $\Phi_{t_t}(\tau)$, and $\Phi_v(\tau)$. At high pressures, the computed correlation function approaches the red dashed line, which neglects all velocity changing elastic collisions. At low pressures, the computed correlation function approaches the blue dot-dashed line, representing the limit where all elastic collisions contribute to the effective damping.

where the present acetylene measurements were made, the ensemble average of the elastic collisions results in nearly full dephasing at the total collision rate, $\gamma_e + \gamma$. This is consistent with good fits to a Voigt line shape, and a linear pressure dependence of the Lorentzian broadening, as observed experimentally. The slope of HWHM vs. pressure in this region is the total collision rate/ 2π . The line shapes begin to deviate from Voigt forms by 0.1 mbar as

the increasingly fast inelastic damping rate begins to compete with the dephasing between different velocity groups. Eventually, at high enough pressures, the velocity changing collisions have no further incremental effect on the pressure broadening. Our measurement of a sub-Doppler pressure broadening with a slope 3.5 times the value obtained by conventional spectroscopy in Doppler-broadened gaseous samples is consistent with an elastic collision rate 2.5 times larger than the inelastic contribution. The linearity of the Lorentzian fitting parameter up to 0.05 mbar is consistent with a typical Doppler shift per elastic collision of at least 2 MHz, according to this simple model.

IV. DISCUSSION

Using saturation dip laser absorption spectroscopy, we have frequency measured the positions of a number of rotational lines in the $v_1 + v_3$ combination band of acetylene. For the stronger transitions, we were able to determine the effect of self-collisional broadening of the line profiles as the sample pressure was increased. The broadening coefficients determined in the present experiment, see Table I, are all $3.5 - 4\times$ those previously reported in conventional, Doppler-broadened spectroscopic measurements of the same transitions. To account for and understand this observation, we have developed a sub-Doppler soft collision model which takes into account the effect of large cross-section, VCCs in the sample. The correlation function $\Phi_v(\tau)$, Equ. (5), actually accounts for several types of velocity-dependent effects in line shapes. In the absence of VCCs at low pressure it gives the normal Gaussian Doppler broadening when averaged over the thermal velocity distribution. Including the effects of VCCs modifies this ensemble average such that extreme velocity groups in the ensemble tend to become more similar with collisions and slow down dephasing. This is a way of describing Dicke narrowing.^{13,45} In the sub-Doppler case, the initial ensemble of interest is velocity-selected and VCCs broaden the velocity distribution and cause a corresponding line broadening. The particular model detailed here with a symmetric small-angle scattering kernel would not show Dicke narrowing however, as this requires significant excursions in velocity space for each molecule prior to inelastic scattering and a kernel with asymmetric probabilities for decreasing and increasing velocity changes in collisions.

Other reported measurements of molecular sub-Doppler lines have also found 2-4 \times greater pressure broadening coefficients compared to measurements of Doppler-broadened

lines.^{7,8,10–12,23,34,35,46} The most detailed studies of the effects of VCCs on saturated absorption profiles have been in atoms such as Xe,^{5,47} and Rb with He, Ne, Ar and Xe collision partners.⁴³ The extremely strong atomic transitions permit measurements over a wide range of pressures. These studies show the same qualitative behavior as depicted in our model, although pressure-broadening in them is primarily driven by phase interrupting atomic collisions, rather than the rotationally inelastic collisions that dominate molecular systems. At low pressures, the narrow sub-Doppler saturated resonance is observed to have a larger Lorentzian broadening component than calculated, based on the pressure broadening coefficient measured in conventional absorption studies. Line widths are also found to increase with a non-linear pressure dependence: linear at low pressures followed by a region of downward curvature, approaching a high pressure linear region with a slope near the value measured for the Doppler-broadened gas-phase absorption data.

Similar results were seen in methane^{7,9} in early measurements of the 3.39 μm lasing transition. The direct effect of VCCs with increasing pressure can also be seen in the formation of a broad pedestal under the narrow saturation feature under appropriate conditions.⁹ Measurements of vibration-rotation transitions in CO_2 found a γ_{self} for the saturation features that was $2.7\times$ larger than the Doppler-broadened quantity.^{11,12} A similar result for CO_2 was reported earlier by Meyer et al.¹⁰ and incorrectly attributed to a combination of transit time broadening and saturation effects.

Recent measurements of the self-broadening of sub-Doppler spectra of CH_3F in the 3 μm region⁴⁸ are of interest to compare with the present results. Okabayashi et al.⁴⁸ report $\gamma_{self}=9.6(1.3)$ MHz/Torr for the $rQ(7, 4)$ transition, converted to the HWHM quantity, which compares to a value of 10.7(0.5) previously reported by Cartlidge and Butcher⁴⁹ from linear spectroscopy in the Doppler-limited regime. Published data for ammonia^{25,50–52} also find no significant differences between the self-broadening coefficients for Doppler or sub-Doppler broadening. This implies that, for these molecules, the effects of VCCs in the saturation dip experiment are minimal, contrary to the case of acetylene, methane, CO_2 or ethylene, above. The obvious difference is the presence of the dipole moment in CH_3F and NH_3 , causing even long-range collisions to be dominated by dipole-dipole interactions more effective at causing state- or phase-changing transitions than in molecules or atoms without a dipole moment.

These observations are in accord with measurements and modeling of the decay of coherent transients reported by Berman et al.⁵³ Their work investigated the effects of velocity

changing collisions by measurement of photon echo signals following rapid Stark switching of the molecular transition frequency out of resonance with the probe laser frequency. The conclusions were that, in CH_3F , the decay of a Doppler hole created by a narrow band laser is dominated by hard, inelastic, collisions. Further, the measurements were interpreted to show that phase-changing collisions in the absence of state-changing ones, were also of low probability, so that the T_1 and T_2 lifetimes were the same. Much more recent work by Rubtsova et al.^{54,55} confirmed this result. Stark-shifting measurements are only possible on molecules possessing a dipole moment and degenerate or nearly degenerate levels of opposite parity, so cannot be applied to acetylene, for example, where the present results suggest VCCs play a much more significant role.

In related work by the Schwendeman group,^{56–58} collisions in CH_3F were probed by elegant sub-Doppler IR-IR double resonance methods. They observed collisional transfer of velocity spikes characteristic of resonant rotational energy transfer. After such a collisional rotational energy exchange, a new population of a nearby rotational state is formed with the narrow velocity distribution of the initially pumped one, and a corresponding component of the initially tagged level appears to be fully thermalized translationally in a single collision. This special type of collision between indistinguishable particles may of course also be considered, rather than the complete translational thermalization of the tagged quantum state, as a small-angle soft collision, but with an exchange of rotational state labels. In either view, these special energy-elastic self-collisions will contribute to pressure broadening, despite having no observable effect on the energy transfer rates. It is the relative importance of these collisions that is at issue in the current interest in possible ortho/para differences in the pressure broadening of acetylene.^{27,28}

It would be interesting to measure coherent transients in acetylene using a rapid frequency-switching, or transient double resonance, experiment to compare with the present interpretation of the sub-Doppler saturation dip data. Precise understanding of the various contributions to sub-Doppler line profiles are crucial to the interpretation of spectroscopic experiments that attempt to test fundamental theory^{38,59} while information on the rate of VCCs is required for the modeling precise experimental measurements of pressure-broadened lines recorded under Doppler-broadened conditions relevant to remote sensing⁶⁰ and Doppler thermometry.⁶¹

V. SUPPLEMENTARY MATERIAL

Supplementary material consisting of a) compressed files containing LabView[®] executable code and source code libraries to permit readers to implement the model for computing the effects of velocity-changing collisions on sub-Doppler lineshapes described in this paper and b) a pdf document showing the effect of a larger width Gaussian transit-time broadening on the fits to a Voigt profile, may be obtained from the publisher.

VI. ACKNOWLEDGEMENTS

We gratefully acknowledge helpful discussions with Dr Patrick Dupré (Université Littoral Côte d’Opal) and Dr Benoit Darquié, (Université Paris-13). Work at Brookhaven National Laboratory was carried out under Contract No. DE-SC0012704 with the U.S. Department of Energy, Office of Science, and supported by its Division of Chemical Sciences, Geosciences and Biosciences within the Office of Basic Energy Sciences.

REFERENCES

- ¹A. A. Madej, A. J. Alcock, A. Czajkowski, J. E. Bernard, and S. Chepurov, “Accurate absolute reference frequencies from 1511 to 1545 nm of the $\nu_1 + \nu_3$ band of $^{12}\text{C}_2\text{H}_2$ determined with laser frequency comb interval measurements,” *J. Opt. Soc. Am. B* **23**, 2200–2208 (2006).
- ²M. J. Cich, D. Forthomme, C. P. McRaven, G. V. Lopez, G. E. Hall, T. J. Sears, and A. W. Mantz, “Temperature-dependent, nitrogen-perturbed line shape measurements in the $\nu_1 + \nu_3$ band of acetylene using a diode laser referenced to a frequency comb,” *J. Phys. Chem. A* **117**, 13908–13918 (2013), pMID: 24125088, <http://dx.doi.org/10.1021/jp408960e>.
- ³D. Forthomme, M. J. Cich, S. Twagirayezu, G. E. Hall, and T. J. Sears, “Application of the HartmannTran profile to precise experimental data sets of $^{12}\text{C}_2\text{H}_2$,” *J. Quant. Spectrosc. Radiat. Transfer.* **165**, 28–37 (2015).
- ⁴S. Twagirayezu, M. J. Cich, T. J. Sears, C. P. McRaven, and G. E. Hall, “Frequency comb-referenced spectroscopy of ν_4 - and ν_5 -excited hot bands in the $1.51\mu\text{m}$ spectrum of C_2H_2 ,” *J. Molec. Spectrosc.* **316**, 64–71 (2015).

- ⁵P. Cahuzac, E. Marié, O. Robaux, R. Vetter, and P. R. Berman, “The effect of velocity-changing collisions upon saturated absorption profiles: the laser line of xenon at $\lambda = 3.51\mu\text{m}$,” *J. Phys. B. Atom. Molec. Phys.* **11**, 645–651 (1978).
- ⁶C. Bordé, “Progress in understanding sub-Doppler line shapes,” (*Laser Spectroscopy III*, Springer Series in Optical Sciences, Berlin, Heidelberg, 1977) pp. 121–134.
- ⁷S. N. Bagaev, E. V. Baklanov, and V. I. Chebotayev, “Measurement of elastic cross sections in a gas by laser spectroscopy,” *JETP Letts.* **16**, 15–18 (1972).
- ⁸R. L. Barger and J. L. Hall, “Pressure shift and broadening of methane line at $3.39\mu\text{m}$ studied by laser-saturated molecular absorption,” *Phys. Rev. Letts.* **22**, 4–7 (1969).
- ⁹S. N. Bagaev, A. S. Dychkov, and V. Chebotayev, “Investigation of the shape of non-linear resonances at low-pressures,” *JETP Letts.* **29**, 519–523 (1979).
- ¹⁰T. W. Meyer, C. K. Rhodes, and H. A. Haus, “High resolution line-broadening and collisional studies in CO_2 using non-linear spectroscopic techniques,” *Phys. Rev. A* **12**, 1993–2008 (1975).
- ¹¹L. S. Vasilenko, V. P. Kochanov, and V. P. Chebotayev, “Nonlinear dependence of optical resonance widths at CO_2 transitions on pressure,” *Opt. Comm.* **20**, 409–411 (1977).
- ¹²V. P. Kochanov, S. G. Rautian, and A. M. Shalagin, “Impact broadening of resonances involving changes of velocity,” *Z. Eksp. I Teoret. Fiz.* **72**, 1358–1374 (1977).
- ¹³L. Galatry, “Simultaneous effect of Doppler and foreign gas broadening on spectral lines,” *Phys. Rev.* **122**, 1218–1223 (1961).
- ¹⁴S. G. Rautian and I. I. Sobel’man, “The effect of collisions on the Doppler broadening of spectral lines,” *Sov. Phys. Usp.* **9**, 701–716 (1967).
- ¹⁵E. D. Black, “An introduction to Pound- Drever- Hall laser frequency stabilization,” *Amer. J. Phys.* **69**, 79–87 (2001).
- ¹⁶S. Twagirayezu, G. E. Hall, and T. J. Sears, “Quadrupole splittings in the near-infrared spectrum of $(\text{NH}_3)\text{-N-14}$,” *J. Chem. Phys.* **145** (2016), 10.1063/1.4964484.
- ¹⁷O. Axner, P. Kluczynski, and O. Lindberg, “A general non-complex analytical expression for the n th Fourier component of a wavelength-modulated Lorentzian lineshape function ,” *J. Quant. Spectr. Rad.Transf.* **68**, 299 – 317 (2001).
- ¹⁸J. Westberg, J. Wang, and O. Axner, “Fast and non approximate methodology for calculation of wavelength-modulated Voigt lineshape functions suitable for real-time curve fitting,” *J. Quant. Spectr. Rad.Transf.* **113**, 2049–2057 (2012).

- ¹⁹W. Demtröder, *Laser Spectroscopy: Basic Concepts and Instrumentation*, 2nd ed. (Springer-Verlag: Berlin, 1996).
- ²⁰C. Bordé and J. L. Hall, “Ultrahigh resolution saturated absorption spectroscopy,” in *Laser Spectroscopy*, edited by R. G. Brewer and A. Mororadian (Plenum, New York, 1974) pp. 125–142.
- ²¹J. L. Hall, “Sub-Doppler spectroscopy, methane hyperfine spectroscopy and ultimate resolution limits,” in *Méthodes de spectroscopie sans largeur Doppler de niveaux excités de systèmes moléculaires simples* (CNRS, Paris, 1974) pp. 105–125.
- ²²C. Bordé, J. L. Hall, C. V. Kunasz, and D. G. Hummer, “Saturated absorption lineshape: Calculation of the transit-time broadening by a perturbation approach,” *Phys. Rev. A* **14**, 236–263 (1976).
- ²³L.-S. Ma, J. Ye, P. Dubé, and J. L. Hall, “Ultrasensitive frequency-modulation spectroscopy enhanced by a high-finesse optical cavity: theory and application to overtone transitions of C₂H₂ and C₂HD,” *J. Opt. Soc. Amer. B* **16**, 2255–2268 (1999).
- ²⁴P. Dupré, “Dipole saturated absorption modeling in gas phase: Dealing with a Gaussian beam,” *J. Quant. Spectrosc. Rad. Transf.* **205**, 196–212 (2018).
- ²⁵L. S. Rothman, I. E. Gordon, Y. Babikov, A. Barbe, D. C. Benner, P. F. Bernath, M. Birk, L. Bizzocchi, V. Boudon, and et al., “The HITRAN 2012 molecular spectroscopic database,” *J. Quant. Spectrosc. Radiat. Transf.* **130**, 4–50 (2013).
- ²⁶V. P. Chebotayev and V. S. Letokhov, “Nonlinear narrow optical resonances induced by laser radiation,” *Prog. Quant. Electr.* **4**, 111–206 (1975).
- ²⁷K. Iwakuni, S. Okubo, K. M. Yamada, A. Onae, F.-L. Hong, and H. Sasada, “Ortho-para dependent pressure effects observed in the near infrared band of acetylene by dual-comb spectroscopy,” *Phys. Rev. Letts.* **117**, 143902(5) (2016).
- ²⁸K. K. Lehmann, “Influence of resonant collisions on the self-broadening of acetylene,” *J. Chem. Phys.* **146** (2017), 10.1063/1.4977726.
- ²⁹D. Jacquemart, J.-Y. Mandin, V. Dana, L. Regalia, X. Thomas, and P. Von der Hayden, “Multispectrum fitting measurements of line parameters for 5- μ m cold bands of acetylene,” *Journal of Quantitative Spectroscopy and Radiative Transfer* **75**, 297–422 (2002).
- ³⁰M. Kusaba and J. Henningsen, “The $v_1 + v_3$ and the $v_1 + v_2 + v_4^1 + v_5^{-1}$ combination bands of ¹³C₂H₂, linestrengths, broadening parameters and pressure shifts,” *J. Molec. Spectrosc.* **209**, 216–227 (2001).
- ³¹J. Wang, Y. R. Sun, L.-G. Tao, A.-W. Liu, and S.-M. Hu, “Communication: Molecular near-infrared transitions determined with sub-kHz accuracy,” *J. Chem. Phys.* **147**, 091103 (2017).

- ³²W. C. Swann and S. L. Gilbert, “Pressure-induced shift and broadening of 1560–1630 nm carbon monoxide wavelength-calibration lines,” *Journal of the Optical Society of America B* **19**, 2461–2467 (2002).
- ³³O. M. Lyulin, V. I. Perevalov, I. Morino, T. Yokota, R. Kumazawa, and T. Watanabe, “Measurements of self-broadening and self-pressure-induced shift parameters of the methane spectral lines in the 5556-6166 cm^{-1} range,” *J. Quant. Spectrosc. Rad. Trans.* **112**, 531–539 (2011).
- ³⁴M. Wappelhorst, M. Mürtz, P. Palm, and W. Urban, “Very high resolution CO laser spectrometer and first sub-Doppler line-shape studies near 60THz ($5\mu\text{m}$),” *Appl. Phys. B* **65**, 25–32 (1997).
- ³⁵J. Chen, T.-P. Hua, L.-G. Tao, Y. Sun, A.-W. Liu, and S.-M. Hu, “Absolute frequencies of water lines near 790 nm with 10^{-11} accuracy,” *J. Quant. Spectrosc. Rad. Transf.* **205**, 91–95 (2018).
- ³⁶S. Tochitsky and R. Butcher, “Precise measurements of line broadening and line shifts in low-pressure gases using a heterodyne CO_2 laser spectrometer: applications to C_2H_4 and CH_3OH ,” *J. Opt. Soc. Amer. B* **15**, 1392–1398 (1998).
- ³⁷A. N. Goncharov, M. N. Skvortsov, and V. P. Chebotayev, “Study of relaxation of molecular iodine by the method of saturated absorption spectroscopy,” *Appl. Phys. B* **51**, 108–115 (1990).
- ³⁸F. M. J. Cozijn, P. Dupré, E. J. Salumbides, K. S. E. Eikema, and W. Ubachs, “Sub-Doppler frequency metrology in HD for tests of fundamental physics,” *Phys. Rev. Lett.* **120**, 153002 (2018).
- ³⁹Y. Tan, J. Wang, C.-F. Cheng, X.-Q. Zhao, A.-W. Liu, and S.-M. Hu, “Cavity ring-down spectroscopy of the electric quadrupole transitions of H_2 in the 784 - 852nm region,” *J. Molec. Spectrosc.* **300**, 60 – 64 (2014).
- ⁴⁰R. Ciurylo, R. Jaworski, J. Jurkowski, A. S. Pine, and J. Szudy, “Spectral line shapes modeled by a quadratic speed-dependent Galatry profile,” *Physical Review A* **63**, 032507 (2001).
- ⁴¹R. Wehr, R. Ciurylo, F. Thibault, J. R. Drummond, and A. D. May, “Dicke narrowed spectral line shapes of CO in Ar: Experimental results and a revised interpretation,” *J. Molec. Spectrosc.* **235**, 54–68 (2006).
- ⁴²T.-S. Ho and S.-I. Chu, “Collision kernel and interatomic potential,” *Phys. Rev. A* **33**, 3067–3073 (1986).
- ⁴³K. E. Gibble and A. Gallagher, “Measurements of velocity-changing collision kernels,” *Phys. Rev. A* **43**, 1366–1380 (1991).
- ⁴⁴B. H. McGuyer, R. Marsland III, B. A. Olsen, and W. Happer, “Cusp kernels for velocity-changing collisions,” *Phys. Rev. Letts.* **108**, 183202 (2012).
- ⁴⁵R. L. Farrow and R. E. Palmer, “Comparison of motionally narrowed CARS line shapes of H_2 with hard-collision and soft collision models,” *Opt. Letts* **12**, 984–986 (1987).

- ⁴⁶J. Hald, L. Nielsen, J. C. Petersen, P. Varming, and J. E. Pedersen, “Fiber laser optical frequency standard at 1.54 μm ,” *Opt. Expr.* **19**, 2052–2063 (2011).
- ⁴⁷P. Cahuzac, J. L. LeGrouét, P. E. Toschek, and R. Vetter, “Collisional effects upon optical coherences: experimental study in a xenon three-level system,” *Appl. Phys.* **20**, 83–88 (1979).
- ⁴⁸Y. Okabayashi, Y. Miyamoto, J. Tang, and K. Kawaguchi, “Pressure broadening of transitions in the $\text{CH}_3\text{F } \nu_4$ band using Stark modulated Lamb dips,” *Chem. Phys. Letts.* **619**, 144–147 (2015).
- ⁴⁹A. G. Cartlidge and R. J. Butcher, “Self-broadening of transitions in the $\text{CH}_3\text{F } \nu_4$ band using a difference frequency laser,” *J. Phys. B: At. Mol. Opt. Phys.* **23**, 2083–2090 (1990).
- ⁵⁰M. Triki, C. Lemarchand, B. Darquié, P. L. T. Sow, V. Roncin, C. Chardonnet, and C. Daussy, “Speed-dependent effects in NH_3 self-broadened spectra: Towards the determination of the Boltzmann constant,” *Phys. Rev. A* **85**, 062510 (2012).
- ⁵¹A. T. Mattick, A. Sanchez, N. A. Kurnit, and A. Javan, “Velocity dependence of collision-broadening cross section observed in an infrared transition of NH_3 gas at room temperature,” *Appl. Phys. Letts.* **23**, 675–678 (1973).
- ⁵²A. Mattick, N. Kurnit, and A. Javan, “Velocity dependence of collision broadening cross sections in NH_3 ,” *Chem. Phys. Letts.* **38**, 176 – 180 (1976).
- ⁵³P. R. Berman, J. M. Levy, and R. G. Brewer, “Coherent optical transient study of molecular collisions: Theory and observations,” *Phys. Rev. A* **11**, 1668–1688 (1975).
- ⁵⁴D. V. Ledovskikh, N. N. Rubtsova, and V. A. Reshetov, “Collision relaxation in $(\text{CH}_3\text{F})\text{-C-13}$ with buffers,” *Laser Phys. Letts.* **7**, 734–738 (2010).
- ⁵⁵N. N. Rubtsova, V. G. Gol’dort, V. N. Ishchenko, S. A. Kochubei, E. B. Khvorostov, D. V. Ledovskikh, V. A. Reshetov, and I. V. Yevseyev, “Coherent transients in gases,” *Laser Phys.* **21**, 1252–1259 (2011).
- ⁵⁶U. Shin, Q. Song, and R. H. Schwendeman, “Observation of 3-level and collisionally induced 4-level infrared-infrared double-resonance effects in $\text{CH}_3\text{F-c-12}$,” *J. Chem. Phys.* **95**, 3964–3974 (1991).
- ⁵⁷Q. Song and R. H. Schwendeman, “Infrared infrared double-resonance of methyl-fluoride in foreign gases,” *J. Molec. Spectrosc.* **153**, 385–405 (1992).
- ⁵⁸G. M. Soriano and R. H. Schwendeman, “Polarization modulation effects in infrared-infrared four-level double resonance in $\text{CH}_3\text{F-C-13}$ and $\text{NH}_3\text{-N-15}$,” *J. Molec. Spectrosc.* **190**, 294–317 (1998).
- ⁵⁹L.-G. Tao, A.-W. Liu, K. Pachucki, J. Komasa, Y. R. Sun, J. Wang, and S.-M. Hu, “Toward a determination of the proton-electron mass ratio from the Lamb-dip measurement of HD,” *Phys. Rev. Lett.* **120**, 153001 (2018).

⁶⁰N. H. Ngo, H. Tran, and J. M. Hartmann, “An isolated line-shape model to go beyond the Voigt profile in spectroscopic databases and radiative transfer codes,” *J. Quant. Spectrosc. Rad. Transf.* **129**, 89–100 (2013).

⁶¹J. Fischer, B. Fellmuth, C. Gaiser, T. Zandt, L. Pitre, F. Sparasci, M. D. Plimmer, M. de Podesta, R. Underwood, G. Sutton, G. Machin, R. M. Gavioso, D. Madonna Ripa, P. P. M. Steur, J. Qu, X. J. Feng, J. Zhang, M. R. Moldover, S. P. Benz, D. R. White, L. Gianfrani, A. Castrillo, L. Moretti, B. Darquié, E. Moufarej, C. Daussy, S. Briaudeau, O. Kozlova, L. Risegari, J. J. Segovia, M. C. Martn, and D. del Campo, “The Boltzmann project,” *Metrologia* **55**, R1–R20 (2018).